ISSN 0001-4338, Izvestiya, Atmospheric and Oceanic Physics, 2015, Vol. 51, No. 4, pp. 381–390. © Pleiades Publishing, Ltd., 2015.
Original Russian Text © V.I. Kuzin, G.A. Platov, N.A. Lapteva, 2015, published in Izvestiya AN. Fizika Atmosfery i Okeana, 2015, Vol. 51, No. 4, pp. 437–447.

Assessing the Effect of Year-to-Year Runoff Variations in Siberian Rivers on Circulation in the Arctic Ocean[1]

V. I. Kuzin, G. A. Platov, and N. A. Lapteva

Institute of Computational Mathematics and Mathematical Geophysics, Siberian Branch, Russian Academy of Sciences, pr. Akademika Lavrent'eva 6, Novosibirsk, 630090 Russia

e-mail: kuzin@sscc.ru

Received October 6, 2014; in final form, November 14, 2014

Abstract—The propagation of freshwater anomalies from Siberian rivers in the Arctic Ocean in the 21st century has been simulated using a model developed in Institute of Computational Mathematics and Mathematical Geophysics, Russian Academy of Sciences (ICMMG RAS), based on the output of the ICM RAS model and scenario RPC 8.5, project CMIP-5 IPCC. River runoff has been calculated using a linear reservoir model with 1/3-degree resolution, including nine major drainage basins in Siberia.

Keywords: river runoff, Arctic Ocean, North Atlantic, numerical simulation, oceanic circulation, circulation regimes

DOI: 10.1134/S0001433815040064

INTRODUCTION

The Arctic plays an important role in the Earth's climate system. In particular, this is true for the hydrological component of climatic processes in the Arctic and the Arctic Ocean (AO). The interest in these processes has been rapidly growing in the recent decades. The Arctic Ocean accounts for about 11% of the freshwater in the World Ocean [1, 2]. The freshwater content of the AO, evaluated based on estimates in [3–10], is given in [11, 12]. The total freshwater amount, evaluated with respect to the mean salinity value of 34.8 pro mille, is estimated at 80000 m^3 [12] or 74 ± 7.4 thousand km^3 [11].

According to [11], freshwater inflow into the AO can be divided into the following components: the excess of precipitation over evaporation, averaging about 2222 ± 200 km^3 per year [11]; according to most recent estimates, freshwater inflow through the Bering Strait is about 2500 km^3 per year [7, 8]; a decrease in the arctic ice and melting of the Greenland Ice Sheet, caused by climate changes and warming in the Arctic [9]; and river runoff. Pioneer estimates of river-water inflow into the Arctic were given in [4, 13]. Current estimates [11, 12] yield values of about 3200 km^3 per year.

The major rivers of the Russian North discharge about 2240 km^3 per year, which is about 70% of the entire river runoff [12]. The largest contribution is due to the Yenisei, Lena, and Ob [14]. According to data of Hydrometeoservice [15, 16], total annual discharges over the measurement periods show considerable year-to-year variations because of changes in the within-year hydrograph. Freshwater discharge takes place through the Fram Strait and the straits of the Canadian Archipelago. Discharged from the AO into northern Atlantic seas as ice, icebergs, or low-salinity water, freshwater is an important regulator in the formation of the thermohaline structure and meridional circulation of both the North Atlantic and the entire World Ocean [17, 18]. An example of this is the formation of the Great Salinity Anomaly in the 1960s and 1970s [19].

The year-to-year variations of river runoff amount to ±25–35% of its mean values. As follows from [20–22], the variability of atmospheric circulation, the temperature regime, and the surface characteristics play a significant role in those year-to-year variations.

Variations of freshwater propagation in the Arctic Ocean–North Atlantic system were studied in [23] based on a model developed at the Institute of Computational Mathematics and Mathematical Geophysics, Siberian Branch, Russian Academy of Sciences (ICMMG SB RAS).

In addition to year-to-year variations, the hydrological characteristics of Siberian rivers show positive trends which have attracted the attention of climatologists in recent years as they reflect the trends in the general climate system. Thus, river runoff in the Arctic has increased in recent decades [24–27]. According to data in [28], the runoff of the six major Siberian rivers increased by 7% from 1936 to 1999. This increase correlates well with an increase in NAO index [28]. This also can be associated with the positive trend in

[1] The paper is dedicated to the memory of Academician G.I. Marchuk.

NAM (North Annular Mode), which is a part of the Arctic Oscillation [29]. In this context, an important question is whether this process will extend further to the 21st century, producing feedbacks in the climate system. All these facts suggest that the effect of variations of freshwater balance in the Arctic on the climate system in the following century can be considerable, so this effect should be studied based on climate models of river runoff [30–33], circulation models of individual oceans [34–36], and joint models of the climate system of CMIP-5 Project (see, e.g., [37]). The method of mathematical modeling for studying processes in the atmosphere and the ocean, developed by Gurii Ivanovich Marchuk [38], is among the most effective instruments for studying the Earth's climate system. This article considers the results of a simulation of year-to-year changes in freshwater balance, which can take place in the Arctic Ocean in the 21st century against the background of runoff variations of Siberian rivers calculated using a model of ICMMG SB RAS based on the results of simulation by the ICM RAS model for the scenario RCP 8.5, CMIP-5 project.

1. RIVER RUNOFF CALCULATIONS FOR SIBERIAN REGION

1.1. Climate Model of River Runoff

The model being developed is a linear reservoir model. It consists of linear reservoirs or a chain of reservoirs in grid cells. The rate of changes in discharge from a cell in the simplest version of Kalinin–Milyukov model [24, 30] is determined based on the solution of convolution integral (Duhamel).

This specific implementation of the model uses a structure proposed at the Max Planck Institute, Hamburg University [30]. Under this approach, water flow on the land is divided into three components: surface runoff, subsurface runoff, and river runoff. The values of delay factors for surface and river runoffs are determined by formulas reflecting their dependence on cell slope or elevation differential between the cells divided by the distance between their centers. The surface and subsurface runoffs are calculated for individual reservoirs, while the river runoff is calculated for a chain of reservoirs. The number of such chains in river channels is evaluated using a second-order regression polynomial, determined by the delay factor. The value of the delay factor for subsurface runoff in a cell is assumed constant. Water infiltration into the soil was simulated in each cell based on surface characteristics and the percent of the mean soil moisture content derived from hydrological data for each basin. The percent area of wetlands and lakes was taken into account in each cell.

1.2. Data for river Runoff Simulation and Experimental Setup

The domain under consideration covers the area 40° N–80° N, 50° E–170° E. The resolution of the model in numerical experiments with the climate model of river runoff was taken equal to 1/3 degree over both latitude and longitude.

The chosen runoff model option requires the following input parameters to be specified: precipitation, evaporation, transitions from the liquid into the solid phase and vice versa, and infiltration into the soil. During model verification, these data were taken from MERRA reanalysis data for period 1980–2011. The calculation results were compared with the observational data from hydrological gauges of Hydrometeoservice [15, 16] and data of R-ArcticNET [http://www.r-arcticnet.sr.unh.edu/v4.0/index.html]. For calculations in the 21st century, the results of calculations by the ICM RAS model for scenario RCP 8.5, project CMIP-5 IPCC were used.

Calculations with river runoff models comprised two experiments. The first was intended to verify the runoff model. With this in view, numerical experiments with runoff simulation in Siberian rivers were carried out based on MERRA reanalysis data, resulting in the construction of mean climatic annual hydrographs, which were compared with measurement data. The second experiment involved river runoff simulation in the 21st century based on calculations using the ICM RAS model [39].

1.3. Results of River Runoff Simulation

At the first stage, river runoff values were calculated based on MERRA reanalysis data for 1980–2011 with a time step of 6 h. In the presentation of results, the annual climatic runoff hydrographs were divided in accordance with the basins of AO seas into which the river discharges. Thus, the annual hydrograph of the Ob plus the Yenisei accounts for the flow inflow into the Kara Sea. Water inflow into the eastern seas of the AO is the sum of hydrographs of Siberian rivers discharging into the Laptev and East Siberian seas. The Lena hydrograph is represented separately.

The simulated mean climatic annual runoff hydrograph is compared with the annual hydrographs of the Ob and Yenisei rivers in Fig. 1. The difference between the maximal amplitudes is –0.2%. Figure 2 gives a simulated annual hydrograph for the Lena River. The difference between the maximal amplitudes is 6.4%. Figure 3 gives the summarized results of climate hydrograph simulation for eastern rivers. The difference in the maximal amplitude is –5.9%. Spring flood periods coincided in all three cases. The results show the model to be acceptable for calculating the climate runoff of Siberian rivers.

The second stage was a numerical experiment for the 21st century (2006–2100) using data obtained

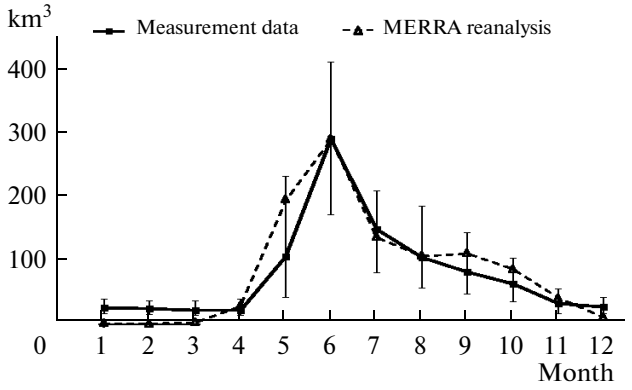

Fig. 1. Mean climatic values of hydrographs for the total runoff of the Ob and Yenisei rivers. The vertical lines show the amplitudes of year-to-year variations in measurement data.

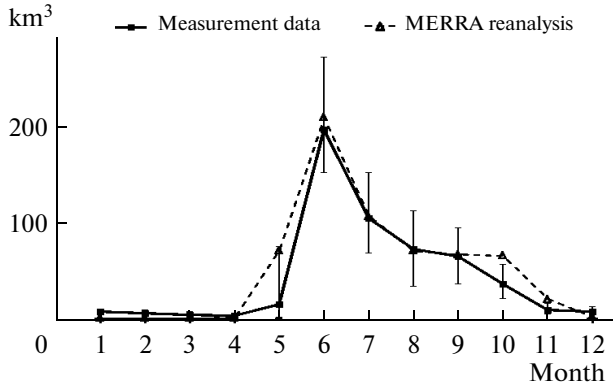

Fig. 2. Climatic values of Lena runoff hydrographs.

from calculations based on the ICM RAS model [39]. The total runoff yields positive inflow values relative to the climatic value of 1798 km^3 per year for the entire period. An analysis of the results for the runoff into different water areas of the AO shows appreciable differences between inflows into the Kara Sea and eastern Arctic seas. In the former case, a deficiency in water input into AO relative to the climatic value of 995 km^3 per year is observed (Fig. 5). After that, the runoff values increase to exceed the climatic values. For rivers flowing into the Laptev and East Siberian seas, the runoff exceeds the climatic value for the entire period (Fig. 6). The runoff here shows a positive linear trend toward its increase in both cases. This trend is more pronounced in eastern rivers. The calculated runoffs were used as data for simulating the dynamics of freshwater balance in the Arctic Ocean by a circulation model.

2. SIMULATION OF HYDROPHYSICAL PROCESSES IN THE ARCTIC OCEAN AND NORTH ATLANTIC

The problem is solved with the use of a regional model of the Arctic and North Atlantic developed in ICMMG SB RAS [36]. The model was developed by improving and localizing a more recent model of the World Ocean [40, 41]. It is based on conventional equations of ocean thermodynamics in curvilinear orthogonal coordinates with the use of hydrostatic and Boussinesq approximations. The model utilizes the method of splitting by physical processes proposed and developed by G.I. Marchuk [42]. The boundary conditions on the surface are specified with the use of a solid lid approximation. In this version of the numerical model, the advection–diffusion operator is split into two operators describing the advection and diffusion processes separately. The horizontal and vertical advection is approximated by the QUICKEST numerical scheme proposed in [43]. The parameterization of vertical turbulence is based on Richardson criterion and a vertical-mixing procedure with the formation of a layer of vertically homogeneous distribution of hydrodynamic characteristics [41]. No salinity restoration is applied on the surface.

The oceanic module is integrated together with the model of elastic viscous-plastic ice CICE 3.14 [44], which is a modification of an earlier Hibler's viscous-plastic model [45]. The ambient characteristics that determine the conditions of ice development included wind velocity, flow velocity of the top oceanic layer, specific moisture content, surface air density and temperature, incoming shortwave and long-wave radiation, the rate of precipitation in the form of rain and snow, ocean surface temperature and salinity, and ocean surface slope. The ice model calculates the following boundary conditions at the ice–water interface: penetrating shortwave radiation; the fluxes of heat, salt, and freshwater; and the friction stress between water and ice.

The characteristics of the lower atmosphere, required to calculate the fluxes of heat and moisture, wind friction stress, and the descending radiation

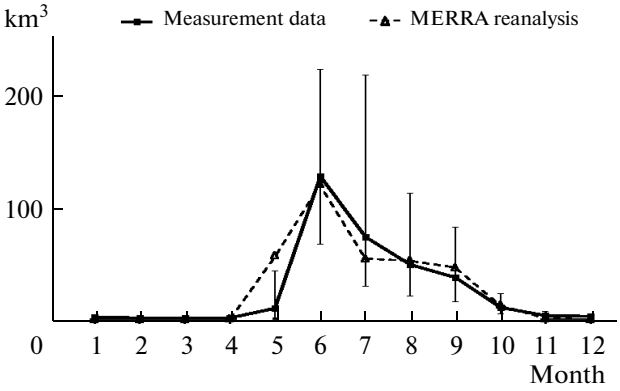

Fig. 3. Climatic values of total runoff hydrographs of eastern rivers.

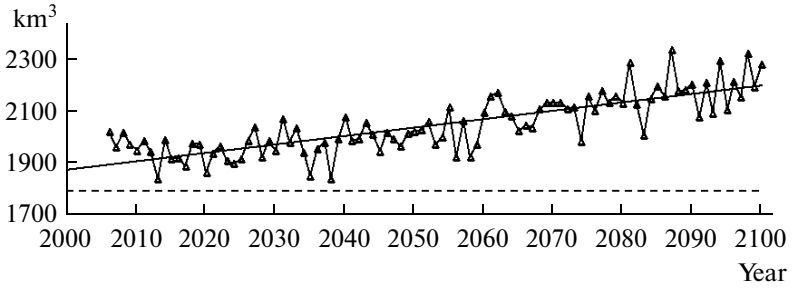

Fig. 4. Year-to-year variations of the total runoff of Siberian rivers into the AO in the 21st century. The full line shows the linear trend in runoff; the dashed line shows the climatic value.

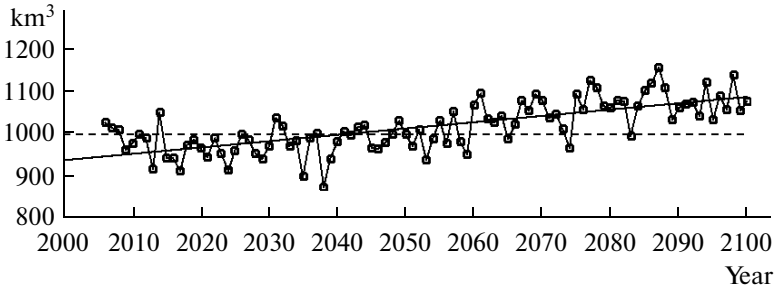

Fig. 5. Total runoff of the Ob and Yenisei into the Kara Sea.

fluxes, were taken from data in CMIP-5 portal, obtained using INMCM4 model ICM RAS for scenario experiment RCP 8.5 covering the period from 2006 to 2100 [39]. The initial distributions of the fields of temperature, salinity, ice thickness, etc., were taken from the results of previous experiments with this model [46] for January 1, 2006.

The numerical grid in the North Atlantic coincides with parallels and meridians with a resolution of $1° \times 1°$. At a latitude of 65° N, this grid turns into a grid for the polar domain, constructed by turning the spherical coordinate system and reprojecting its hemisphere onto the domain above 65° N [47]. The horizontal resolution of the polar grid varies from 14 to 55 km. In the vertical direction, the grid consists of 38 levels with a maximal resolution of 5 m in the top 20-m layer. The minimal depth at the shelf is 20 m. The position of the coastal line is approximated with the maximal accuracy with horizontal resolution taken into account.

The model domain incorporates the Arctic basin and the North Atlantic starting from 20° S. Water temperature and salinity near the Gibraltar Strait is calculated basing on seasonal distributions [48]. The model takes into account the inflow of 52 major rivers in the regions, the most important being the equatorial Amazon and Congo rivers, as well as the largest Siberian Yenisei, Lena, and Ob rivers. Data on the mean seasonal runoff of those rivers were derived from hydrological gauge observations [49]. Moreover, as was noted, according to estimates [11], the total inflow of continental waters in the Arctic amounts to about 3200 km^3/year (about 0.1 Sv), while the major rivers discharge as little as 2456 km^3/year. Therefore, to

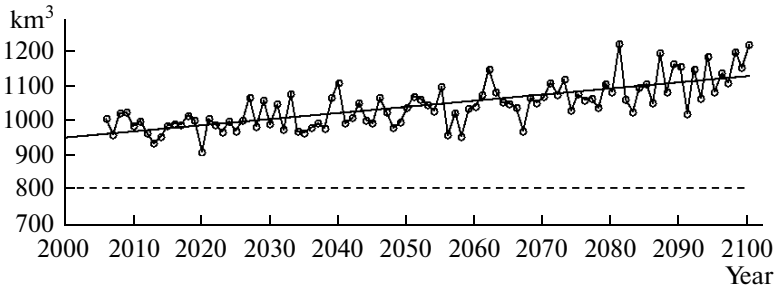

Fig. 6. Total river runoff into the Laptev and East Siberian seas.

obtain the full runoff, the discharge of all rivers involved was multiplied by a factor of 1.3.

The boundary conditions on the bed and solid side boundaries specify zero heat and salt fluxes through those boundaries. The bottom friction is proportional to the bottom flow velocity squared; the no-slip condition is introduced on the side boundaries. The southern boundary at the latitude of 20° S is liquid, implying free advection when the velocity is directed southward, i.e., out of the model domain; otherwise, we have transport from beyond the domain, where the temperature and salinity are determined based on mean monthly data [48]. The boundary condition at river mouths specifies zero-salinity water inflow. The boundary condition for the stream function is assumed constant along the coastal line with increments when crossing the Bering Strait or a river mouth, corresponding to the discharge of the strait or the river. The condition on the southern boundary specifies the discharge compensating for the total inflow of all rivers in the rest of the domain and water input through the Bering Strait. The barotropic velocity of water outflow is assumed constant along the entire boundary, corresponding to a linear distribution of the stream function. Since the southern boundary of the domain is inaccessible for ice, no additional conditions are specified on the liquid boundary. The Bering Strait is assumed closed for ice motion.

2.1. Numerical Experiments and Results

Two calculations were carried out with the above regional model to evaluate the future contribution of year-to-year runoff variations of Siberian rivers. In the first case, climatic discharge, based on data of [12, 49], was specified for all rivers in the region of the Arctic and North Atlantic; in the second case, in addition to those data, a discharge derived from the results of the second experiment of river runoff calculation was specified for Siberian rivers separately. The comparison of the results of those two calculations yields an estimate of the contribution of the year-to-year variations of the runoff of Siberian rivers to the overall freshwater balance of the Arctic. A description of those calculations should begin with the general pattern of circulation in the Arctic Ocean.

2.2. Characteristic of the General Circulation

The previous experience in simulating circulation in the 20th century shows that the major features of this circulation are associated with the atmospheric effect, which is external with respect to the ocean–ice system. The specific features of the atmospheric motion can be expressed in terms of the values of atmospheric oscillation indices. Commonly, the applications associated with the Arctic region consider two indices, i.e., the index of North Atlantic Oscillation (NAO) and the index of Arctic oscillation (AO). For the 20th century, both indices were evaluated based on

Fig. 7. Oscillation indices: (a) North Atlantic (NAO) and (b) Arctic (AO), according to a forecast of ICM RAS model for 2006–2100 for scenario RCP 8.5, calculated for December–January–February–March and averaged over 5-year time intervals.

data of instrumental measurements; however, their evaluation in the 21th century requires the use of results of scenario-based calculations. Basing on an analysis of the pressure field at the sea level from the ICM RAS model [39] obtained under scenario RCP 8.5 of IPCC project, the time variations of the deviation of the pressure difference between the Azores high and Icelandic low from its mean value yields a forecast of the time variation of NAO index (Fig. 7a). In the period of 2006–2100, the index is generally positive in its first half (up to 2060) with maximums in periods 2015–2030 and 2040–2060 and negative in period 2070–2095 with an appreciable increase in the last 5 years of the 21st century. The AO index, unlike the NAO index, is not directly associated with two observation points; it expresses the maximal difference between the anomalous value of the same sign near the Northern Pole and anomalous values of

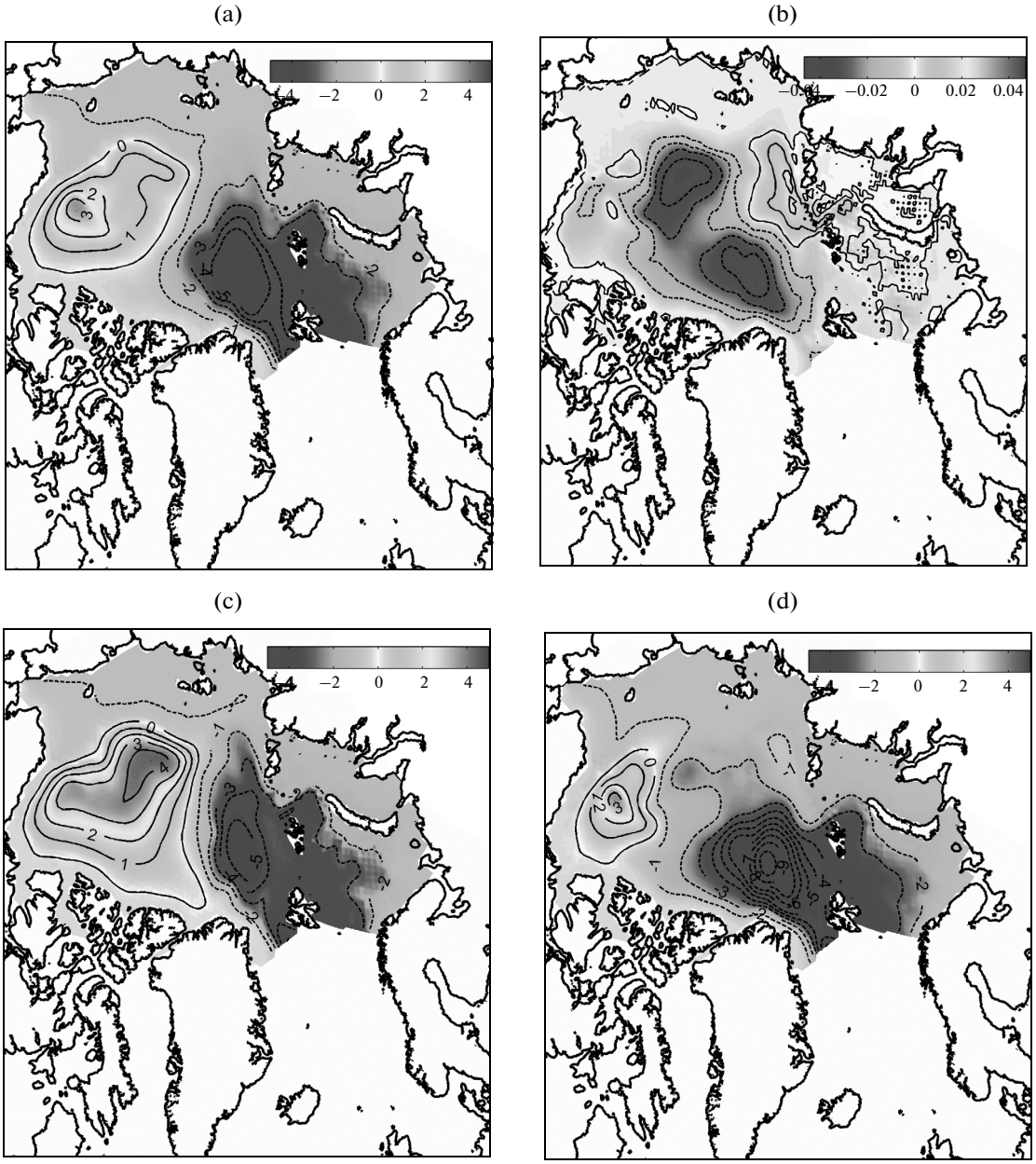

Fig. 8. Stream function (Sv): (a) mean for the experiment, (b) the first mode of singular expansion, (c) the sum of the mean for the experiment and the first mode of singular expansion taken with a coefficient equal to –90% of the maximum for experiment, (d) sum of the mean for the experiment and the first mode of singular expansion taken with a coefficient equal to +90% of the maximal for experiment.

the opposite sign within the latitude range 37°–45° of the Northern Hemisphere. The time variations of the index thus constructed are given in Fig. 7b. Its values are generally positive in the first half of the 21st century and negative in its second part. The correlation between the NAO and AO indices is about 73%, which confirms numerous signs of their interchangeability (see, e.g., [50]).

The response of oceanic circulation to a direct atmospheric impact can be expressed in terms of stream function variations. A singular expansion of the time variations of the vector of state of barotropic ocean shows that the time variations of the expansion coefficients for the first four expansion modes correlate with the time variations of NAO and AO indices according to the table, from which it follows that the first expansion mode is the most sensitive to variations of the indices. Figure 8a shows the spatial distribution of the mean value of the stream function over 2006–2100, and Fig. 8b gives the eigenfunction of the first mode of singular expansion. The spatial distribution of the stream function, corresponding to ±90% of the maximal contribution of the first mode, is given in Figs. 8c and 8d. The former (Fig. 8c) shows the pattern

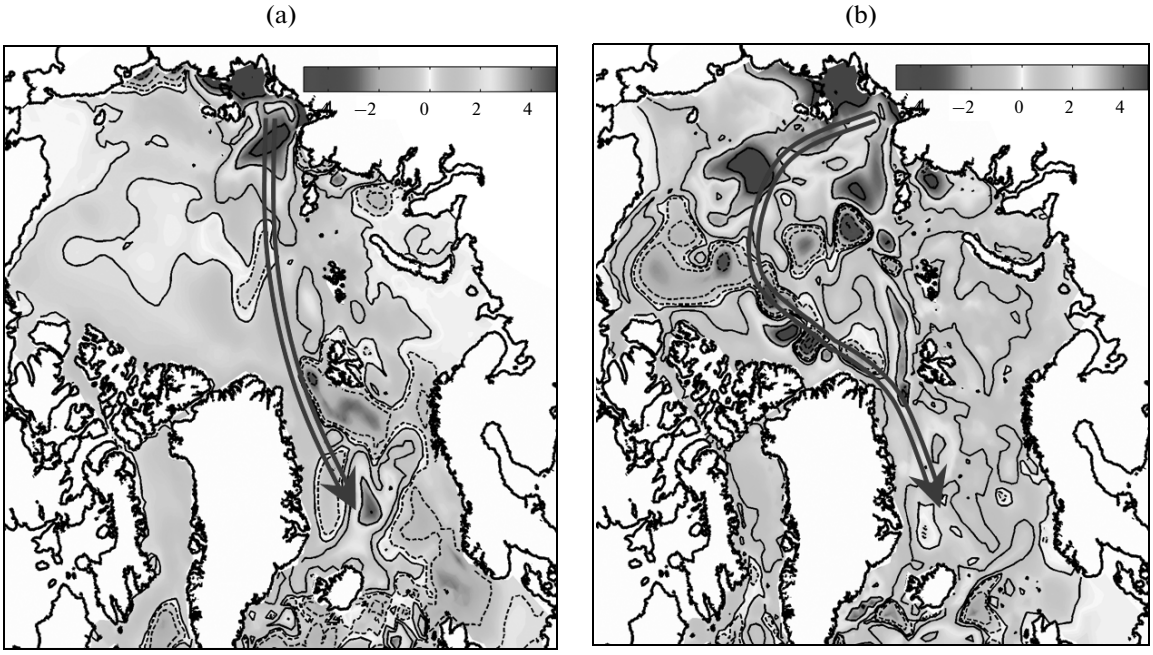

Fig. 9. Pattern of propagation of freshwater anomalies: (a) in the period of positive NAO (AO), year of 2027, and (b) in the period of negative NAO (AO), year of 2073, according to a forecast by ICM RAS model for period 2006–2100, according to scenario RCP 8.5. The full contours correspond to positive values of the anomaly; the dashed contours correspond to negative values.

of the stream function corresponding to a period of positive NAO (AO) index, while the latter (Fig. 8d) shows that to a period of negative index. The contribution of the following modes is less than 40% of variations of the stream function.

When the index is positive, the cyclonic circulation of Atlantic water dominates only in the Amundsen basin, and the Lomonosov ridge separates the cyclonic and anticyclonic circulations in the Arctic. At a negative index, the domain of cyclonic circulation is concentrated in the European part of the Amundsen basin and within the American part of the Canadian basin and the Beaufort Sea. At the same time, the Atlantic water, part of which spread through the Barents Sea and another part through the Fram Strait and along the continental slope, does not move along the slope toward the Laptev Sea but turns aside from the slope and move toward the Canadian Basin immediately after the St. Anna trough.

This pattern of circulation is somewhat different from those we found before in the analysis of variations in the second half of the 20th century [23, 46]. The distinction mostly consists in the different character of circulation at negative atmospheric indices. This is because, in the case of scenario forcing, the period of negative indices coincides with a period when there is no perennial ice, i.e., starting from about 2050, the ice field becomes seasonal and disappears almost completely during the summer season. Thus, the atmospheric effect, which in the 20th century manifested itself through the ice and snow cover, will reach the ocean directly in the second half of the 21st century.

The second half of the 21st century differs from its first half also in that the freshwater anomalies that form here in the first half of the century have different signs in the first and second calculations in the first half (plus in the eastern seas and minus in the Kara Sea), while both anomalies are positive in the second half of the century.

2.3. Propagation of Freshwater Anomaly

The most rapid changes caused by anomalous runoff of Siberian rivers propagate with a velocity of barotropic waves [51], which in our case, with a solid-lid approximation and the representation of barotropic motions in terms of stream function, implies instantaneous propagation. However, the advective propagation of the anomaly and the consequences it has is the most interesting.

According to the two schemes of water circulation in AO, the propagation of a freshwater anomaly can also take place in two ways. The difference of freshwater concentration between the second and first calculation can be expressed in terms of the excess of freshwater concentration Δ. This is the thickness of the freshwater layer that is to be removed for the distribution of one salinity value to become equivalent to the distribution of the other. In the case of freshwater deficiency, the value of Δ is negative.

Figure 9a gives an anomaly of 2027, when a phase of positive circulation indices took place. The export of deviations of freshwater concentration from the perturbation region (the Kara and the Laptev seas)

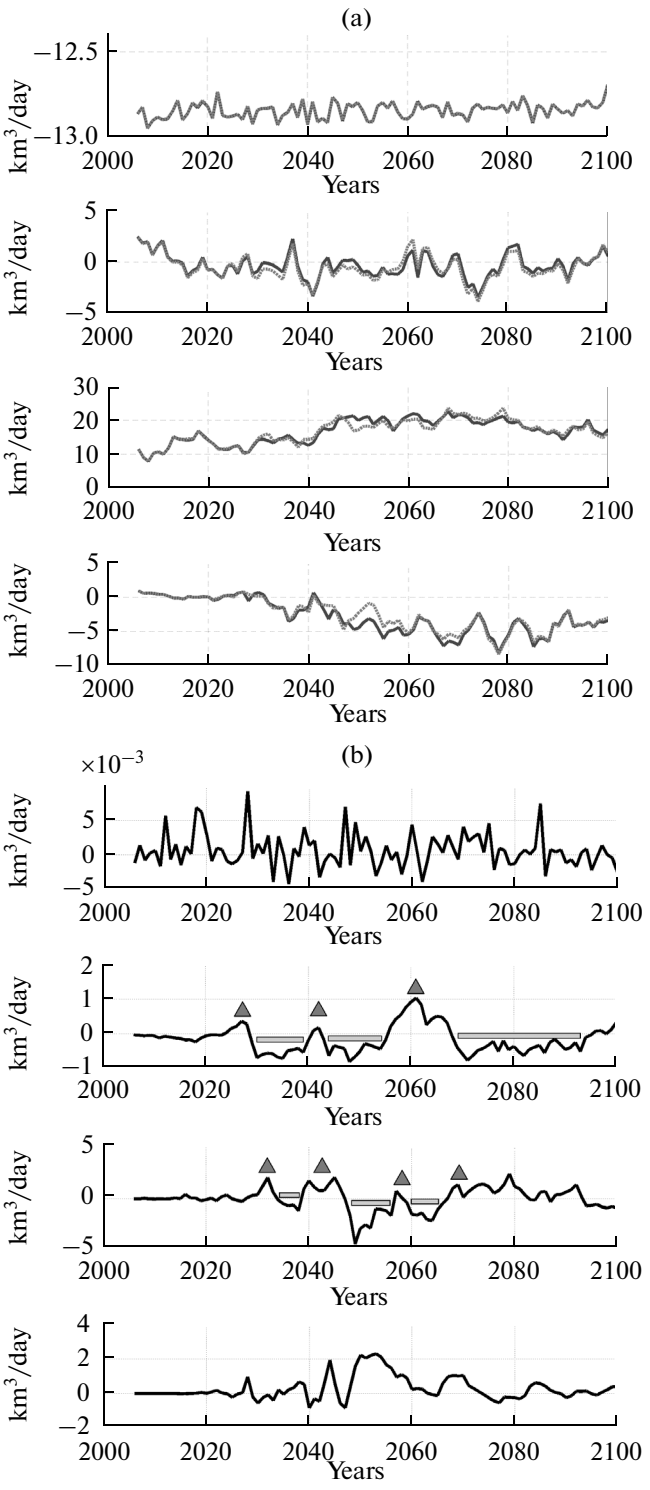

Fig. 10. (a) Mean annual rate of freshwater export from the Arctic in liquid and solid fraction: the solid line corresponds to the first calculation and the dashed line correspond to the second calculation; (b) the difference between the second and first calculation. The panels are arranged in the vertical direction in the following order: the top panel corresponds to discharges through the Bering Strait and the next panel corresponds to discharges through Canadian straits, further are discharges through the Fram Strait, and the bottom panel is for discharges through the Barents Sea.

Coefficients of correlation of the time variations of NAO and AO indices with time variations of the amplitudes of the first four modes in the singular expansion of the barotrophic circulation of the Arctic Ocean

Mode	NAO	AO
1st	−0.4382	−0.6794
2nd	−0.0817	−0.4197
3rd	0.4478	0.1839
4th	−0.1096	0.0975

toward the Fram Strait takes place nearly along the straight line connecting those two regions, because of transpolar drift and propagates further along the southern Greenland coast into the Atlantic. In 2073, the phase of circulation indices was negative, so the trajectory of freshwater anomalies corresponds to stream function contour lines for this period (Fig. 9b).

Figure 10a gives the export of Arctic freshwater through the Bering Strait, the straits of the Canadian Arctic Archipelago, the Fram Strait, and through the Barents Sea. The export through the Bering Strait is negative, thus corresponding to a reverse process, i.e., the import of freshened Pacific water. The freshwater inflow is specified constant, equal to 12.8 km^3 per day with the complete absence of the input of the solid fraction, i.e., ice. This is because this strait is a boundary of a domain where total inflow with a mean annual discharge of 0.8 Sv is specified and a rigid boundary exists for ice. The largest is the export through the Fram Strait, most of it (about 2/3) being the liquid fraction. Part of this export returns through the Barents Sea because of winds and wind currents. The export through Canadian straits is also mostly in the form of liquid fraction, since the passage of ice through narrow straits is limited.

Figure 10b shows the difference between the calculation results with the use of obtained discharges of Siberian rivers and the results based on climatic values of discharges. The positive deviations of discharge in the Fram Strait, showed in the figure by triangles, take place in the first years of abrupt changes in atmospheric circulation indices from maximal positive to negative values. Those bursts are followed by periods of negative deviations of discharges, shown in the figure by horizontal strips. Similar deviations occur in discharges through Canadian straits, though their amplitude is much less and the period of the negative anomaly is longer. This implies that, according to the results of these calculations, the appearance of a positive anomaly of freshwater export through the Fram Strait is compensated for by the subsequent negative anomaly, as well as a deceleration or even reverse of freshwater export through Canadian straits.

CONCLUSIONS

The climate changes that have been taking place on the Earth in the recent decades have the most significant effect in the high latitudes of the Northern Hemisphere. To describe such changes is a very complicated problem, requiring many factors to be taken into account, including ice formation and melting, the inflow of Atlantic and Pacific waters, the formation of deep-sea waters, and northern river runoff.

The developed model of climatic river runoff was used to carry out experiments for simulating river runoff based on MERRA reanalysis data and calculations with the use of ICM RAS model with scenario RCP 8.5, IPCC Program [39]. The comparison of the simulated total values of annual hydrograph with data of measurements at hydrological gauges on Siberian rivers shows a good agreement in terms of the amplitudes and occurrence phases of spring and summer floods. While showing common positive trends, the simulated year-to-year variations in the 21st century feature considerable differences between inflows into the Kara Sea and the eastern Arctic seas. The model runoff increases in accordance with precipitation, which can be a response to climate changes in Siberia leading to an increase in the runoff of Siberian rivers in recent decades. In the 21st century, the inflow into the Kara Sea up to 2040 is less than the climatic value, while freshwater inflow into eastern seas is in excess of the climatic value for the 20st century, leading to a difference between the anomalies in freshwater distribution in AO.

An analysis of the results of numerical simulation of freshwater propagation in the Arctic shows that the role of freshwater anomalies becomes most significant in the periods of rapid changes in atmospheric circulation. According to the results obtained with the model of ICM RAS, such changes take place in 2030, 2042, 2057, and 2070, resulting in an increase in freshwater export through the Fram Strait with the subsequent compensating decrease. Similar, albeit much lesser, changes take place in the freshwater export through Canadian straits.

ACKNOWLEDGMENTS

This study was supported by the Russian Foundation for Basic Research, project no. 14-05-00730; Presidium of RAS, project 23.3; Branch of Mathematics, RAS, project 1.3.3.-6.; and project 109 IP SO RAS.

REFERENCES

1. V. V. Ivanov, "Water balance and water resources of the Arctic region," Tr. Arkt. Antarkt. Nauchno-Issled. Inst. **323**, 4–24 (1976).
2. I. A. Shiklomanov, A. I. Shiklomanov, R. B. Lammers, et al., "The dynamics of river water inflow to the Arctic Ocean," in *NATO Sci. Ser., 2: Proc. of the NATO Advanced Research Workshop on the Freshwater Budget of the Arctic Ocean* (Kluwer, Tallinn, 2000), pp. 281–296.
3. *World Ocean Atlas*, Vol. 3: *Arctic Ocean*, Ed. by S. G. Gorshkov (Pergamon, New York, 1983).
4. *Atlas of the Arctic*, Ed. by A. F. Treshnikov (Arkt. Antarkt. Nauchno-Issled. Inst., Moscow, 1985) [in Russian].
5. D. J. Hanzlik and K. Aagaard, "Fresh and Atlantic water in the Kara Sea," J. Geophys. Res **85** (C9), 4937–4942 (1980).
6. R. W. McDonald, C. S. Wong, and P. E. Erickson, "The distribution of nutrience in the southeastern Beaufort Sea: Implications for water circulation and primary production," J. Geophys. Res. **92** (C3), 2939–2952 (1987).
7. R. A. Woodgate, K. Aagaard, R. D. Muench, et al., "The Arctic Ocean boundary current along the Eurasian slope and the adjacent Lomonosov Ridge: Water mass properties, transports and transformations from moored instruments," Deep Sea Res. Part I **48**, 1757–1792 (2001).
8. R. A. Woodgate, K. Aagaard, and T. Weingartner, "Interannual changes in the Bering Strait fluxes of volume, heat, and freshwater between 1991 and 2004," Geophys. Res. Lett. **33**, L15609 (2006). doi 1029/2006GL026931
9. E. Linacre and B. Geerts, The Arctic: the ocean, sea ice, icebergs, and climate (1998). http://www-das.uwyo.edu/~geerts/cwx/notes/chap17/arctic.html.
10. C. L. Parkinson, J. C. Comiso, H. J. Zwally, et al., *Arctic Sea Ice, 1973-1976: Satellite Passive-Microwave Observations* (NASA, Washington, D.C., 1987).
11. M. C. Serreze, A. P. Barrett, A. G. Slater, et al., "The large-scale freshwater cycle of the Arctic," J. Geophys. Res. **111** (C11010), 1–19 (2006). doi 10.1029/2005JC003424
12. K. Aagaard and E. C. Carmack, "The role of sea ice and other fresh water in the arctic circulation," J. Geophys. Res. **94** (C10), 14485–14498 (1989).
13. J. D. Milliman and R. H. Meade, "World wide of river delivery sediment to the oceans," J. Geol. **91**, 1–21 (1983).
14. A. Dai and K. Trenberth, "Estimates of freshwater discharge from continents: Latitudinal and seasonal variations," J. Hydrometeorol. **3**, 660–687 (2002).
15. *Long-Term Data on the Regime and Resources of Surface Continental Waters*, Part 1 (Gidrometeoizdat, Leningrad, 1985), Nos. 10, 12, and 16 [in Russian].
16. *Annual Data on the Regime and Resources of Surface Continental Waters 1981–1990*, Part 1, Vol. 1 (Novosibirsk), Vol. 10 (Krasnoyarsk), Vol. 16 (Yakutsk) [in Russian].
17. S. S. Lappo, "On the sources of northward heat advection through the equator in the Atlantic Ocean," in *Study of Ocean–Atmosphere Interaction Processes* (Gidrometeoizdat, Moscow, 1984), pp. 125–129 [in Russian].
18. W. S. Broecker, "Thermohaline circulation, the Achilles heel of our climate system: Will man-made CO_2 upset the current balance?," Science **278**, 1582–1586 (1997).
19. R. R. Dickson, J. Meincke, S.-A. Malmberg, and A. J. Lee, "The "Great Salinity Anomaly" in the

Northern North Atlantic 1968–1982," Prog. Oceanogr **20** (2), 103–151 (1988).

20. J. E. Walsh, "Global atmospheric circulation patterns and relationships to Arctic freshwater fluxes," in *The Freshwater Budget of the Arctic Ocean*, Ed. by E. L. Lewis, E. P. Jones, P. Lemke, et al. (Kluwer, Norwell, MA, 2000), pp. 21–41.
21. D. W. J. Thompson and J. M. Wallace, "Annular modes in extratropical circulation. Part 1: Month-to-month variability," J. Clim. **13**, 1000–1016 (2000).
22. D. W. J. Thompson, J. M. Wallace, and G. C. Hegerl, "Annular modes in extratropical circulation. Part 2: Trends," J. Clim. **13**, 1018–1036 (2000).
23. V. I. Kuzin, G. A. Platov, and E. N. Golubeva, "Influence that interannual variations in Siberian river discharge have on redistribution of freshwater fluxes in Arctic Ocean and North Atlantic," Izv., Atmos. Ocean. Phys. **46** (6), 770–783 (2010).
24. D. A. Burakov, "Estimation of linear runoff parameters," Meteorol. Gidrol. **10**, 89–95 (1989).
25. D. Yang, D. L. Kane, L. D. Hinzman, et al., "Siberian Lena River hydrologic regime and recent change," J. Geophys. Res. **107** (D23), 4694 (2002). doi 10.1029/202JD002542
26. J. W. McClelland, R. M. Holmes, B. J. Peterson, and M. Stieglitz, "Increasing river discharge in the Eurasian Arctic: Consideration of dams, permafrost thaw, and fires as potential agents of change," J. Geophys. Res. **109**, D18102 (2004). doi 10.1029/2004JD004583
27. S. Berezovskaya, D. Yang, and D. Kane, "Compatibility analysis of precipitation and runoff trends over the large Siberian watersheds," Geophys. Res. Lett. **31** (2004). doi 10.1029/2004GL121277
28. B. J. Peterson, R. M. Holmes, J. W. McClelland, et al., "Increasing river discharge to the Arctic Ocean," Science **298**, 2171–2173 (2002).
29. H. Ye, D. Yang, T. Zhang, et al., "The impact of climatic conditions on seasonal river discharges in Siberia," J. Hydrometeorol. **5**, 286–295 (2004).
30. S. Hagemann and L. Dumenil, *Hydrological Discharge Model, Tech. Rep. 17* (MPI, Hamburg, 1998).
31. V. Ch. Khon and I. I. Mokhov, "The hydrological regime of large river basins in Northern Eurasia in the XX–XXI Centuries," Water Resour. **39** (1), 1–10 (2012).
32. V. I. Kuzin and N. A. Lapteva, "Mathematical simulation of climatic river discharge from the Ob–Irtysh basin," Atmos. Oceanic Opt. **25** (6), 440–445 (2012).
33. V. I. Kuzin and N. A. Lapteva, "Mathematical simulation of the runoff of main Siberian rivers," Opt. Atmos. Okeana **27** (6), 525–529 (2014).
34. V. I. Kuzin, *The Finite Element Method in the Modeling of Oceanic Processes* (Comput. Cent. Sib. Branch Russ. Acad. Sci., Novosibirsk, 1985) [in Russian].
35. V. I. Kuzin, E. N. Golubeva, and G. A. Platov, "Simulation of the hydrophysical characteristics of the Arctic Ocean–North Atlantic system," in *Fundamental Studies of Oceans and Seas*, Vol. 1, Ed. by N. P. Laverov (Nauka, Moscow, 2006), pp. 166–190 [in Russian].
36. E. N. Golubeva and G. A. Platov, "On improving the simulation of Atlantic water circulation in the Arctic Ocean," J. Geophys. Res. **112**, C04S05 (2007). doi 10.1029/2006JC003734
37. V. P. Dymnikov, V. N. Lykosov, and E. M. Volodin, "Problems of modeling climate and climate change," Izv., Atmos. Ocean. Phys. **42** (5), 568–585 (2006).
38. G. I. Marchuk and A. S. Sarkisyan, *Mathematical Modeling of Ocean Circulation* (Nauka, Moscow, 1988) [In Russian].
39. E. M. Volodin, N. A. Diansky, and A. V. Gusev, "Simulation and prediction of climate changes in the 19th to 21st centuries with the Institute of Numerical Mathematics, Russian Academy of Sciences, model of the Earth's climate system," Izv., Atmos. Ocean. Phys. **49** (4), 347–366 (2013).
40. A. Proshutinsky, R. H. Bourke, and F. A. McLaughlin, "The role of the Beaufort Gyre in Arctic climate variability: Seasonal to decadal climate scales," Geophys. Res. Lett. **29** (2002). doi 10.1029/2002GL015847
41. E. N. Golubeva, Yu. A. Ivanov, V. I. Kuzin, and G. A. Platov, "Numerical simulation of the World Ocean circulation taking into consideration the upper quasi-homogeneous layer," Okeanologiya (Moscow) **32** (3), 395–405 (1992).
42. G. I. Marchuk, *Numerical Solution of Problems of Atmospheric and Oceanic Dynamics* (Gidrometeoizdat, Leningrad, 1974) [in Russian].
43. B. P. Leonard, "A stable and accurate convective modeling procedure based on quadratic upstream interpolation," Comput. Methods Appl. Mech. Eng. **19**, 59–98 (1979).
44. E. C. Hunke and J. K. Dukowicz, "An elastic–viscous–plastic model for sea ice dynamics," J. Phys. Oceanogr. **27** (9), 1849–1867 (1997).
45. W. D. Hibler, "A dynamic thermodynamic sea ice model," J. Phys. Oceanogr. **9** (4), 815–846 (1979).
46. E. N. Golubeva and G. A. Platov, "Numerical modeling of the Arctic Ocean ice system response to variations in the atmospheric circulation from 1948 to 2007," Izv., Atmos. Ocean. Phys. **45** (1), 137–151 (2009).
47. R. J. Murray, "Explicit generation of orthogonal grids for ocean models," J. Comput. Phys. **126**, 251–273 (1996).
48. M. Steele, R. Morley, and W. Ermold, "PHC: A global hydrography with a high quality Arctic Ocean," J. Clim. **14** (9), 2079–2087 (2000).
49. C. J. Vörösmarty, B. M. Fekete, and B. A. Tucker, Global River Discharge, 1807–1991, Version 1.1 (RivDIS), Data Set (Oak Ridge National Laboratory Distributed Active Archive Center, Oak Ridge, Tennessee, USA, 1998). https://daac.ornl.gov/cgi-bin/dataset_lister.pl?p=16. doi 10.3334/ORNLDAAC/199
50. M. H. P. Ambaum, B. J. Hoskins, and D. B. Stephenson, "Arctic Oscillation or North Atlantic Oscillation," J. Clim. **14**, 3495–3507 (2001).
51. V. B. Zalesny and V. O. Ivchenko, "Modeling the global circulation response and the regional response of the Arctic Ocean to the external forcing anomalies," Oceanology (Engl. Transl.) **50** (6), 829–840 (2010).

Translated by G. Krichevets